UNIVERSITY OF LEEDS

This is a repository copy of *Performance Evaluation of Pulse Width Modulation Techniques for Losses Reduction in Modular Multilevel Flying Capacitor Converter*.

White Rose Research Online URL for this paper:
http://eprints.whiterose.ac.uk/99418/

Version: Accepted Version

eprints@whiterose.ac.uk
https://eprints.whiterose.ac.uk/

Performance Evaluation of Pulse Width Modulation Techniques for Losses Reduction in Modular Multilevel Flying Capacitor Converter

O.J.K. Oghorada *, L. Zhang *†*

*School of Electronic and Electrical Engineering, University of Leeds, United Kingdom,
el11oo@leeds.ac.uk, l.zhang@leeds.ac.uk

Keywords: Phase-shifted-PWM, Phase-disposed-PWM, Hybrid-PWM, Modular multilevel flying capacitor converter and power losses

Abstract

This paper presents the analysis and evaluation of power losses in a modular multilevel flying capacitor converter (MMFCC) controlled by three different pulse width modulation techniques. A new unipolar hybrid PWM scheme, which combines phase disposed PWM (PD-PWM) and phase shifted PWM (PS-PWM), is proposed. Detailed electrical and thermal models of the single star configured FC cells are implemented and simulated using MATLAB/SIMULINK and PLECS. The conduction and switching losses of semiconductor devices and power losses of floating capacitors in the simulated MMCC are evaluated. The results show that the proposed PWM scheme gives the lowest overall power losses and hence the highest efficiency of the three methods under different modulation index variations. Furthermore, the quality of the voltage waveform of the proposed method is as good as that obtained by using PS-PWM.

1 Introduction

The current and future changes in power systems due to interfacing of renewable energy sourced power generators and interconnection of multi-national power systems have led to the active development of power converters for medium and high-power application. Most studies have focused on the modular multilevel cascaded converters (MMCC) [1] for their modular structure, flexibility in scale up or down to meet voltage requirement and good waveform performances at lower switching frequencies. Conventional module concepts comprise both the two-level half bridge (2L-HB) and full bridge (2L-FB) and nomenclature adopted in [2] classifies the MMCC's based on their cell structure as double and single configured cells (either as star or delta). Another module concept investigated is based on the full-bridge three-level flying capacitor converter (3L-FCC) and is presented in [3] for STATCOM application.

Apart from circuit structure another important aspect for MMCC is the PWM schemes. Various modulation techniques have been studied for MMCC's including space vector PWM[4, 5], phase-disposition PWM (PD-PWM) [6] and phase-shifted PWM (PS-PWM) [3, 7]. Most of these studies are mainly concerned with their ability in achieving good output waveform performances measured by Total Harmonic Distortion (THD) factor, and maintaining module and floating capacitor (for 3L-FCC) voltage balances. Few have dealt with such important issues as their effects on power losses of the MMCC and on the loss distributions which determine temperature differences between individual semiconductor devices and modules. Some publications have reported power loss studies in MMCC using 2L-HB and 2L-FB modules [8-10] but not controlled by PWM schemes. There is no work in the literature investigating power loss in the 3L-FCC module-based MMCC's.

This paper presents a study which evaluates power losses of a 3L-FCC module (figure 1(a)) when it is controlled respectively by three different PWM techniques; namely PD-PWM, PS-PWM and a new unipolar hybrid PWM (PSPD-PWM) schemes. It is well-known that PD-PWM is the most preferred technique for 2L-HB and 2L-FB module-based MMCCs compared to the other multilevel PWM schemes. This is because it generates the least power losses due to very low device switching loss whilst still maintains high waveform quality. However, as will be shown in the paper, the result is different when PD-PWM is applied to 3L-FCC, the low switching losses may still be kept but its control causes inner flying capacitor voltages fluctuate resulting in increased distortion in the output voltage waveform. This, in turn, leads to high losses in the equivalent series resistance (ESR) in the flying capacitors and poor THD.

The paper is organized as follows; section II present the 3L-FCC module as the building block of the single star MMCC. Section III, the principles of the three modulation methods and section IV describes the power loss evaluation. This model integrates the devices (switch and diodes) and flying capacitor power loss calculations with electro-thermal models of the devices. To verify the validity of the proposed hybrid technique for MMFCC, simulation results are presented under same load, modulation index and switching frequency conditions in relation to both PD and PS-PWM schemes.

2 Flying Capacitor Converter-MMCC

The basic module of an FCC-MMCC is a three-level full bridge flying capacitor converter (3L-FCC). Figure 1 shows a single phase limb consisting of two such modules. As can be seen each 3L-FCC module has 8 switch-diode pairs, a module and two voltage clamping capacitors, C_{DC}, C_{xn}, C_{xn}', where **x** refers to phase arms **a**, **b** or **c** and **n**, = **1** or **2** labels the module

position on each phase arm, hence forming four cells. The voltage on C_{DC} defines the module voltage rating as V_{DC} and this value, together with the capacitance, is twice that of the two floating capacitors. The 3L-FCC modules generate five voltage levels, i.e. V_{DC}, $V_{DC}/2$, **0**, $-V_{DC}/2$, $-V_{DC}$ using its 16 switching states. These are realized by selecting the route of current flow, either by connecting or by-passing floating capacitors. Switch pairs in each of the four cells shown in the left hand side (LHS) of figure 1 as $(S_{a11}:S_{a14})$, $(S_{a12}:S_{a13})$, $(S_{a11}':S_{a14}')$ and $(S_{a12}':S_{a13}')$ must obviously be complementary, which limits the valid switching states for this module to a total of 16.

To use this topology in a three phase system, three phase limbs can be wired in either star or delta connection. Using the classification of [2], figure 2 shows a single star Flying Capacitor cell.
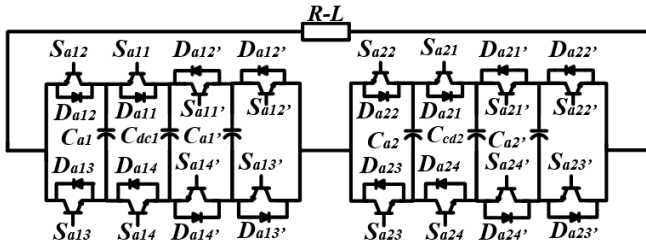
Figure 1: Two cascaded 3L-FCC modules
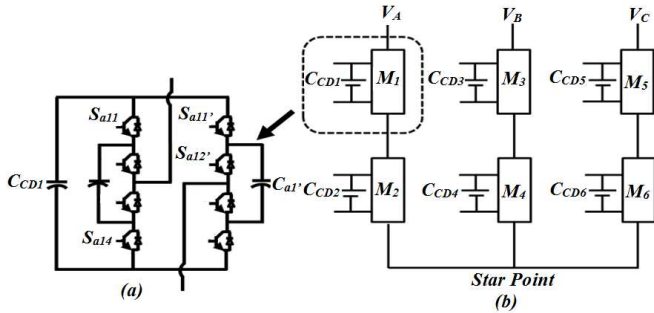
Figure 2: Circuit diagram of (a) flying capacitor module and (b) three-phase six module 3L-FCC inverter in star connection, named SSFCC-MMCC

3 The PWM Control Techniques

These techniques are based on comparison of multi-carrier signals with either a single (bipolar) or two reference sinusoidal signals (unipolar) to synthesize pulse trains to control power switches of the MMFCC.

3.1 Unipolar Phase Shifted Pulse Width Modulation

Multiple carrier signals are applied for this PWM technique, two for each module in the chain. For the example of a phase limb with two stacked modules shown in figure 1, there are four carrier signals of equal amplitude and frequency and equal relative phase shifts angle as shown in figure 3(a). This number of carrier waves is equal to number of voltage levels **m**, minus 1 **(m-1)**. The constant phase angle between carriers is given by

$$\alpha_c = \frac{\pi}{N_T} \tag{1}$$

where N_T is the total number of triangular carriers, and in this example, $\alpha_c = 45^0$.

The **50Hz** sinusoidal reference signal and its anti-phase counterpart are compared with the carriers and the intersection points determine the switching times. This arrangement is referred to as unipolar phase shift PWM. The choice of the modulation frequency ratio, **M_f**, being either odd or even integer of the fundamental harmonic component eliminates even harmonics from being predominant in the output voltage waveform Fourier spectrum analysis. In this example **M_f** is chosen to be **5**.

The MMFCC have four cells in each module, so for example of two stacked modules both LHS ($S_{a11}:S_{a14}$, $S_{a12}:S_{a13}$, $S_{a11}':S_{a14}'$, $S_{a12}':S_{a13}'$) and RHS ($S_{a21}:S_{a24}$, $S_{a22}:S_{a23}$, $S_{a21}':S_{a24}'$, $S_{a22}':S_{a23}'$). The pulse trains generated by the intersection of the two reference signals with the carrier waves are identical but phase shifted by α_c. When applied to the switches on LHS and RHS, the floating capacitor voltages maintain their nominal values within a cycle as illustrated in figure 3. The synthesized pulses in figure 3(b) and 3(c) control the switches on the LHS and RHS respectively.
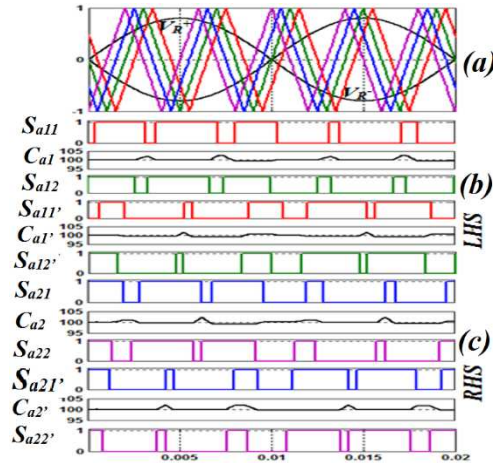
Figure 3: Phase shifted PWM for MMFCC phase-leg illustrating (a) Reference and carrier waveforms for PS-Modulation Technique ;(b) Switching pulses for module 1 (LHS) and(c) Switching pulses for module 2 (RHS)

3.2 Unipolar Phase Disposition Pulse Width Modulation

The phase-disposed PWM scheme uses triangular carrier waveforms that are offset in voltage (i.e. vertically) instead of time (horizontal displacement). The scheme again uses two carrier waveforms for each module in the chain. Four carrier signals are used in implementing this method for the two-module SSFCC-MMCC (figure 4), and these are equally spread across both positive and negative halves of the positive reference signal.

These carrier waveforms are again compared with both positive and negative sinusoidal reference signals to synthesize the pulse trains. When applied to the switches on LHS and RHS, the floating capacitor voltages do not maintain their nominal values within a cycle as illustrated in figure 4. This voltage drift results from the lack of symmetry of the pulse

trains applied across the FCC switches. The $\mathbf{M_f}$ is similar to the PS-PWM counterpart. The pulse trains of figure 4(b) are applied to the switches on the LHS, and those of figure 4(c) to the RHS.
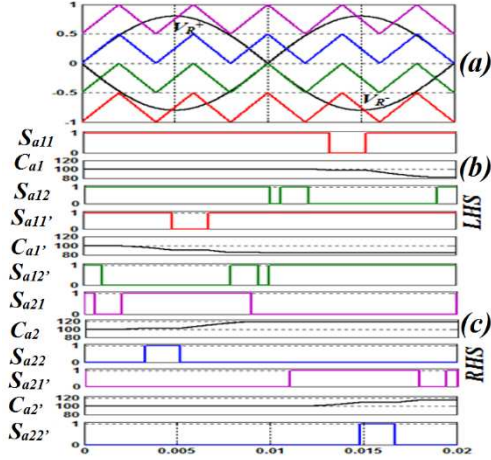
Figure 4: Phase disposed PWM for MMFCC phase-leg illustrating (a) Reference and carrier waveforms for PD-Modulation Technique ;(b) Switching pulses for module 1 (LHS) and(c) Switching pulses for module 2 (RHS)

3.3 Unipolar Hybrid Pulse Width Modulation

This new hybrid PWM technique combines the attributes of the phase disposition and phase shifted methods. Using again $\mathbf{m–1}$ triangular carrier signals ($\mathbf{m} = 5$, the number of voltage levels), these are implemented with half of them equally distributed over each side of the modulating reference signal. The carrier signals above and below the zero value of the reference signals have equal amplitude and frequency. They are also phase shifted from each other; this phase shift angle depends on the voltage level of the converter.

The hybrid PWM technique is implemented for the two-module MMFCC by using four carriers, with two carriers disposed to both positive and negative sides of the reference signal. Carriers above and below the zero point of the reference signal are phase shifted by 90^0. These carriers are compared with a sinusoidal positive and negative reference signal to generate switching signals. The pulse trains applied to individual modules are identical but phase shifted. This symmetry of the pulse trains enables the flying capacitor voltages to maintain their rated values as seen in figure 5.

4 Flying Capacitor Converter-MMCC Losses

Power losses in the MMCC result mainly from the semiconductor devices (IGBT and diodes) and the flying capacitors' equivalent series resistance (ESR). These losses are classified as conduction and switching losses (turn-on and turn-off loss). The off-state leakage loss is not considered here. A combination of IGBT and diode is implemented as a bidirectional switch.

4.1 Conduction Loss

Generally, conduction losses can be evaluated either through simulations fed with precise curve fit data for device on state voltage as a function of current [8, 9] or analytical method based on linear characteristics to achieve average conduction losses [10]. The on-state voltage drop is expressed as

$$V_{cond}(i_{cond}) = V_{ceo} + R_{ON} \cdot i_{cond} \qquad (2)$$

where $\mathbf{V_{cond}}$ is the forward voltage drop, $\mathbf{R_{ON}}$ is either the IGBT or diode on-state resistance, $\mathbf{V_{ceo}}$ denotes either the IGBT on-state zero current collect emitter voltage or zero current diode forward voltage and $\mathbf{i_{cond}}$ is the instantaneous value of converter phase current. These voltage drops result to on-state power dissipation when load current flows through the device. The on-state power loss is clearly dependent on both the conduction current and junction temperature of the device.
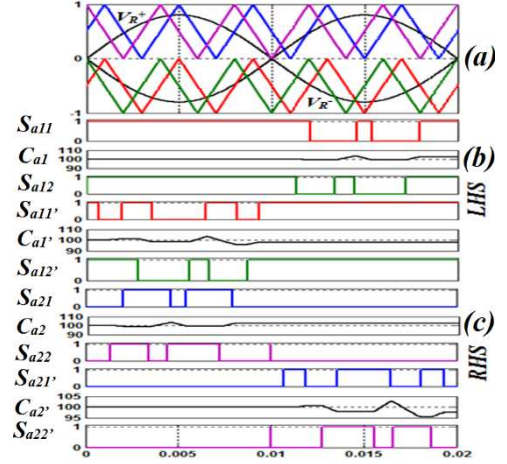
Figure 5: Hybrid-PWM for SSFCC-MMCC phase-leg illustrating (a) Reference and carrier waveforms for Hybrid-Modulation Technique ;(b) Switching pulses for module 1 (LHS) and(c) Switching pulses for module 2 (RHS)

The above formula can be simplified for expressing any semiconductor device on-state forward voltage drop characteristics as

$$V_{cond}(t) = f_{cond}(i_{cond}(t), T_j(t)) \qquad (3)$$

where the forward voltage drop $\mathbf{V_{cond}}$, can be written as $\mathbf{V_{ce}}$ for IGBT and $\mathbf{V_f}$ for diode voltage. Likewise $\mathbf{I_{cond}}$ is the current through the device and can be notated as $\mathbf{i_c}$ for IGBT and $\mathbf{i_f}$ for diode.

The conduction energy loss within a switching period is

$$E_{cond} = \int_{t_0}^{t} i_{cond}(t) \cdot V_{cond}(t) dt \qquad (4)$$

Where $\mathbf{E_{cond}}$ refers to the conduction energies of either IGBT or diode, $\mathbf{t_0}$ to $\mathbf{t}$ is the conduction period.

The average conduction power losses in a device are a function of both the switching frequency $\mathbf{f_{sw}}$ and $\mathbf{E_{cond}}$

$$P_{avg\_cond} = f_{SW} \cdot E_{cond} \qquad (5)$$

where $\mathbf{P_{avg\text{-}cond}}$ can be depicted as either $\mathbf{P_{avg\text{-}condT}}$ (IGBT) or $\mathbf{P_{avg\text{-}condD}}$ (diode) respectively.

4.2 Switching Losses

The switching transition power losses are due to the finite time taken for a semiconductor device to turn from on to off states and vice versa. The power losses are dependent on the type of load, the load current and voltage values, and the duration of

the switching interval which ranges from a few nanoseconds to microseconds. It is impractical to evaluate switching power losses using sampled data over such a short time interval. In this work the switching losses are accounted for by adding an energy impulse after each turn ON and OFF event. $\mathbf{E_{sw}}$ represents the turn ON, turn OFF and reverse recovery energies ($\mathbf{E_{sw\text{-}onT}}$, $\mathbf{E_{sw\text{-}offT}}$ and $\mathbf{E_{rec\text{-}D}}$) of IGBTs and diodes.

The switching loss P_{SW} is calculated as

$$P_{SW} = f_{SW}(E_{sw\_ON} + E_{sw\_OFF}) \tag{6}$$

$$E_{sw\_ON} = f_{SW\_ON}(i_c(t), T_j(t)).(\frac{V_{ce}}{V_{ce\_Ref}}) \tag{7}$$

$$E_{sw\_OFF} = f_{SW\_OFF}(i_c(t), T_j(t)).(\frac{V_{ce}}{V_{ce\_Ref}})$$
$$+ f_{SW\_OFF}(i_f(t), T_j(t)).(\frac{V_f}{V_{f\_Ref}}) \tag{8}$$

Where $\mathbf{V_{ce\_Ref}}$, $\mathbf{V_{f\_Ref}}$ are the reference voltage for switching losses derived from datasheets. $\mathbf{E_{SW\_ON}}$ is turn-on energy for IGBT, $\mathbf{E_{SW\_OFF}}$ is the turn-off energy for IGBT including diode reverse recovery loss, $\mathbf{f_{sw}}$ is the switching frequency and $\mathbf{f_{SW\text{-}ON}}$, $\mathbf{f_{SW\text{-}OFF}}$ are the switching energy function for turn-on and turn-off energies respectively.

4.3 Flying Capacitor Losses

Losses in the flying capacitors of the MMFCC are accounted for by their equivalent series resistance (E.S.R) during both charging and discharging periods. The capacitor energy loss $\mathbf{E_{cap}}$ is expressed as:

$$E_{cap} = \int_{t_0}^{t} C^2 (\frac{dv}{dt})^2.(ESR)dt \tag{9}$$

for the FC a charge/discharge transitions occurring between times $\mathbf{t_0}$ and $\mathbf{t}$. The FC average power loss is calculated as

$$P_{avg\_cap} = f_{SW}.E_{cap} \tag{10}$$

5 Power Loss Estimation Model Of MMFCC

The conduction losses for switching devices in the MMCC can be evaluated from the measured current and temperature values and conduction period according to equations (3), (4) and (5). In this work characteristic curves for the relationship between $\mathbf{I_C}$, $\mathbf{T_{j\text{-}T}}$ and $\mathbf{V_{ce}}$ for the IGBT are taken from the device data sheet [11] as in figure 6(a) and embedded in the power loss calculation model as look-up tables. Look–up tables for diode on-state voltage are also embedded in the model. As illustrated in figure 6(a), these look-up tables enable evaluation of device conduction saturation voltages ($\mathbf{V_{ce}}$ and $\mathbf{V_f}$) at two different device junction temperatures (25°C and 125°C) for measured conducting current. Voltage values are estimated by interpolation for current and temperature values not in the table. The switching energy losses due to IGBT and diodes sequences are evaluated using (6), (7) and (8). The curves shown in figure 6(b) give characteristics of switching energy losses for IGBTs given different values of device current and applied voltage at two IGBT junction temperatures (125°C and 150°C). These form another set of look-up tables which are also embedded in the loss model.

Using the outputs generated from the above energy evaluation procedure, a power calculation algorithm aggregates both Conduction and switching losses over a whole cycle for each IGBT and diode.

(a)

(b)
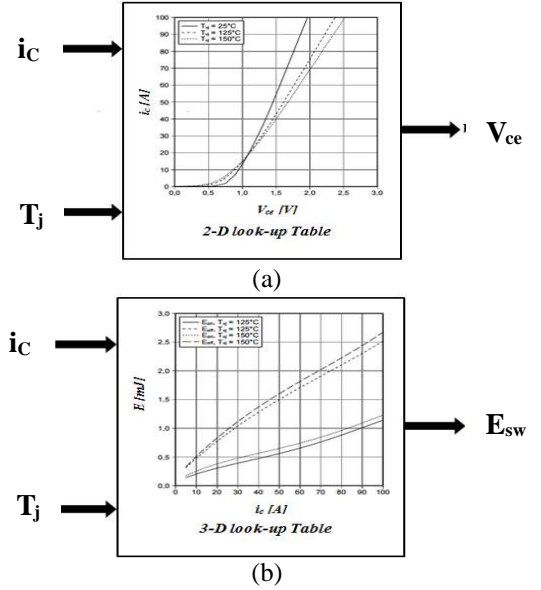
Figure 6: Characteristic curves for (a) $\mathbf{i_c}$ and $\mathbf{T_j}$ vs $\mathbf{V_{ce}}$ and (b) $\mathbf{i_c}$ and $\mathbf{T_j}$ vs $\mathbf{E_{sw}}$

(a)

(b)
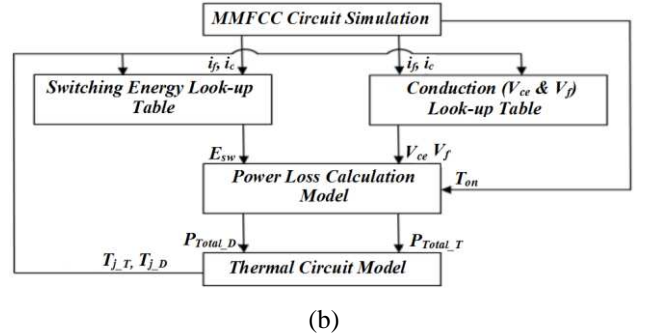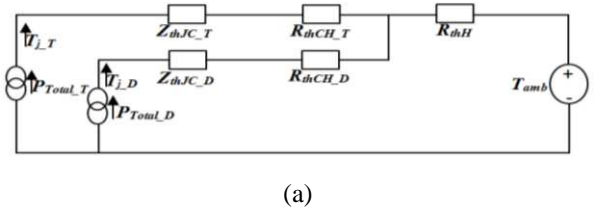
Figure 7: (a) Thermal and (b) loss evaluation model for an SSFCC-MMCC

Having obtained the average power loss values for each device, the results are fed into a thermal circuit model to determine the device junction temperature $\mathbf{T_j}$. This model takes the thermal impedance values of a device from data sheet, including junction to case ($\mathbf{R_{thJC}}$), case to heat sink ($\mathbf{R_{thCH}}$), and heat sink to ambient (($\mathbf{R_{thH}}$) terms. It also requires the measured ambient temperature. Figure 7(a) shows the structure of the thermal circuit model for a device pack consisting of a diode and an IGBT, as they operate under the same load and environmental conditions. Once the newly evaluated junction temperatures are obtained they are fed to the power loss evaluation procedure described above, so repeating the whole process.

Note this whole process starts from power loss evaluation with the device initial junction temperature set to the ambient value. Figure 7(b) shows the block diagram of the loss evaluation model applied to an MMFCC under different PWM modulation schemes.

Components	Description
Load inductor **L**	15.4mH
Resistive load **R**	10Ω
Flying capacitor C_{xn}	C=560µF, E.R.S=0.266Ω
DC link Voltage/module	200V
IGBT module	Infineon F4-50R06W1E3 V_{CES}=600V
Active power **P**	53KW

Table 1: MMFCC Parameters

6   POWER LOSS ANALYSIS

To assess the performance of these three modulation strategies, each was tested in simulation using the same **R-L** load and other parameters as specified in Table 1. The current flowing through one pair of complementary IGBT switches (S_{a11}& S_{a14}) are 'measured' and the waveforms due to the switching pulses generated by the three PWM techniques are as illustrated in figure 8(a)-(c). Each of the switches operates for one half cycle of the fundamental period. Referring to switching pulses due to hybrid PWM in figure 5 the currents through S_{a11} and S_{a14} (in figure 8(a)) show that both having the same current magnitude. S_{a11} switches actively in the first half cycle showing pulsed waveform, while S_{a14} is off. During the second half cycle S_{a14} is on constantly, S_{a11} off. In contrast the current waveforms shown in figure 8(b) for PS scheme shows both switches operate actively in the same pattern during their respective conducting periods. The current waveforms in figure 8(c) from PD scheme bear similar pattern as that by hybrid scheme in figure 8(a) but differs only with the operating duration of S_{a11} (PD) which is shorter compared to its hybrid counterpart, hence S_{a11} switches actively while S_{a14} stays on for the whole half cycle period.

The above current waveforms through the pair of complementary switches in a cell dictate the device power losses in an MMFCC, including conduction and switching losses. Comparisons of these losses for three PWM schemes are shown in figure 9(a) and (b). As can be seen in terms of conduction losses both the hybrid and PS schemes are fractionally higher than the PD scheme. Their loss values are similar due to that the conduction area for current flowing through the devices over a fundamental period is approximately equal. Switching losses for the hybrid scheme is significantly lower than the PS which is the highest. The PS switching transitions performed across the MMFCC switches per fundamental switching period is eight times (figure 3) compared to the four (figure 5) and two (figure 4) generated by the hybrid and PD schemes respectively. The power losses across the FC's of the MMFCC are showed in figure 9(c), these losses are accounted for by the voltage fluctuation which is a function of the current flowing in and out the capacitor

(charging/discharging) and its **E.S.R** value. In this the PD scheme dissipates significantly higher losses across the capacitor due to the large voltage variation experienced during operation in comparison to the other two (figure 10(a)). Combining the above three factors, the hybrid scheme has shown giving the lowest overall losses as shown in figure 9(d), hence it is the most efficient control scheme amongst the three. The waveform performances due to the three schemes are also studied and results in terms of the output voltage THDs are compared as seen figure 10(b)-(d). It is seen that the hybrid scheme (figure 10b) gives similarly low THD values to those of the PS method (figure 10(c)). The PD gives the worst performance due to large FC voltage variation (figure 10(d)). Thus in terms of losses and waveform performance, the proposed hybrid scheme is the most preferred technique.
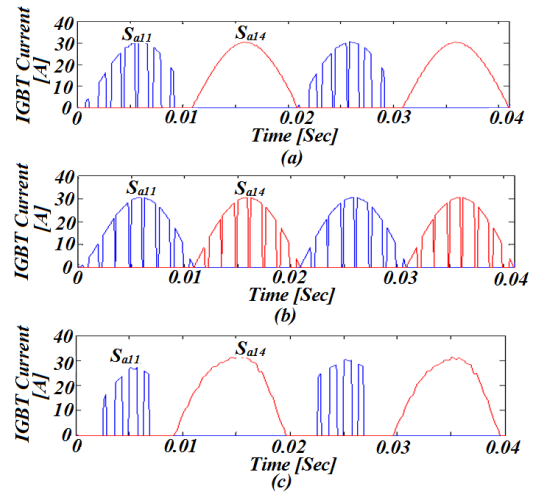
Figure 8: IGBT current across complementary switches for (a) Hybrid, (b) PS and (c) PD schemes

5
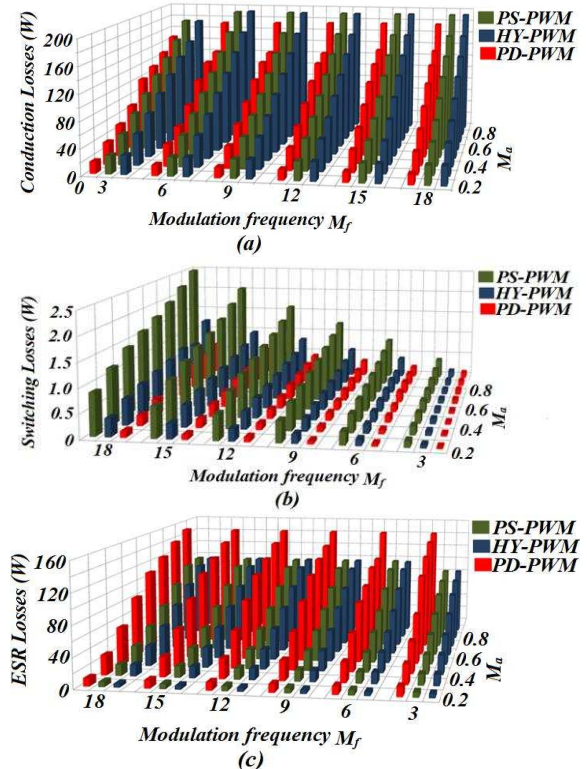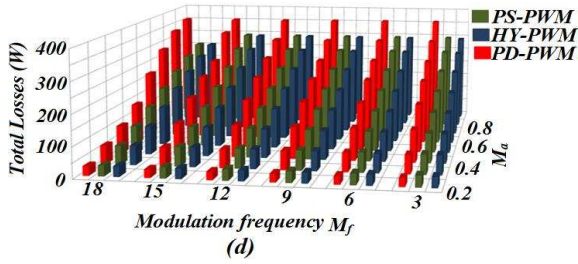
Figure 9: MMFCC Power losses of (a) conduction, (b) switching, (c) FC losses and (d) Total losses
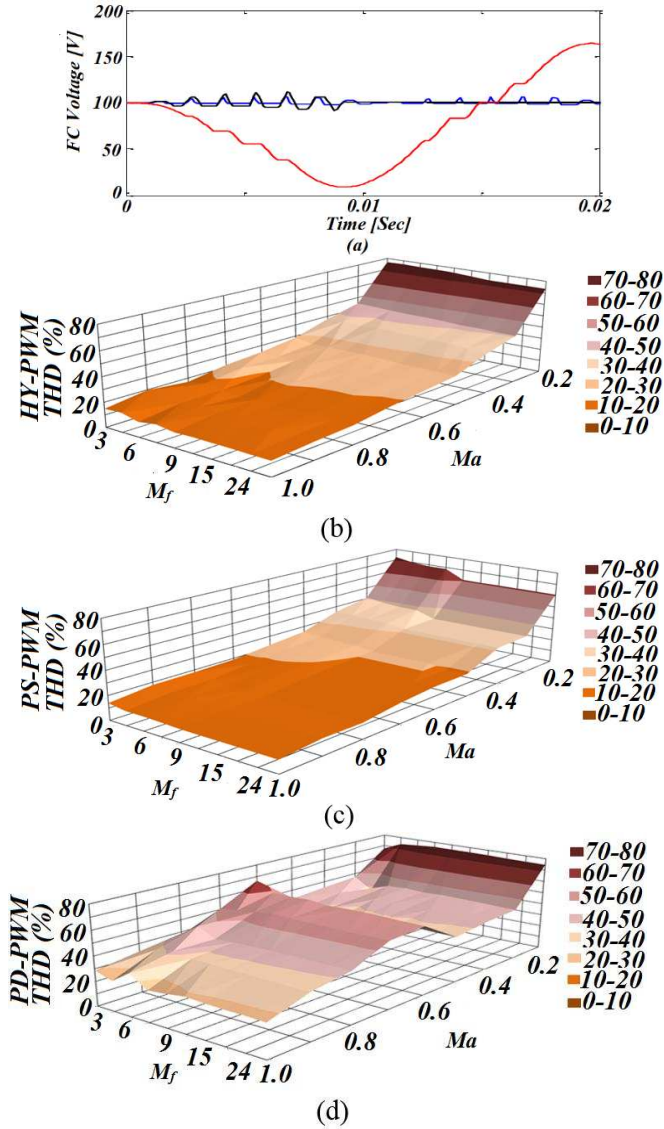
Figure 10: (a) FC voltage fluctuation across three modulation techniques, PD (red), PS (blue) and Hybrid (black), and Fourier Spectrum Analysis of voltage waveform (b) Hybrid-PWM, (c)PS-PWM and (d)PD-PWM.

7 CONCLUSION

A detailed investigation of power losses for an MMFCC has been described in this paper. The overall performance in terms of power loss and waveform quality has been assessed when using the PD, PS modulation schemes and a new modulation technique of hybrid PWM which combines the previous two.

The first of these has good performance regarding the switching losses while the second gives good results in minimizing the FC losses. However it has been demonstrated by extensive simulation that the hybrid technique achieves a good compromise solution. It reduces the switching losses compared with the PS method and reduces the FC losses, and improves output waveform quality, as compared to the PD scheme.

8 Reference

[1] Marquardt, R. and A. Lesnicar. A new modular voltage source inverter topology. in Conf. Rec. EPE. 2003.

[2] Akagi, H., Classification, Terminology, and Application of the Modular Multilevel Cascade Converter (MMCC). Power Electronics, IEEE Transactions on, 2011. **26**(11): p. 3119-3130.

[3] Efika, I.B., C.J. Nwobu, and L. Zhang. Reactive power compensation by modular multilevel flying capacitor converter-based STATCOM using PS-PWM. in Power Electronics, Machines and Drives (PEMD 2014), 7th IET International Conference on. 2014.

[4] Efika, I.B., et al. An overlapping multi-hexagon space vector modulation scheme for modular multilevel cascade converters. in Power Electronics and Applications (EPE), 2013 15th European Conference on. 2013.

[5] Brando, G., et al. A SVM technique with homopolar voltage control in m-level multi modular converters. in Power Engineering, Energy and Electrical Drives (POWERENG), 2013 Fourth International Conference on. 2013. IEEE.

[6] Saeedifard, M. and R. Iravani, Dynamic Performance of a Modular Multilevel Back-to-Back HVDC System. Power Delivery, IEEE Transactions on, 2010. **25**(4): p. 2903-2912.

[7] Hagiwara, M. and H. Akagi, Control and experiment of pulsewidth-modulated modular multilevel converters. Power electronics, IEEE Transactions on, 2009. **24**(7): p. 1737-1746.

[8] Oates, C. and C. Davidson. A comparison of two methods of estimating losses in the Modular Multi-Level Converter. in Power Electronics and Applications (EPE 2011), Proceedings of the 2011-14th European Conference on. 2011.

[9] Li, J., et al. Loss calculation method and loss characteristic analysis of MMC based VSC-HVDC system. in Industrial Electronics (ISIE), 2013 IEEE International Symposium on. 2013. IEEE.

[10] Jones, P.S. and C.C. Davidson. Calculation of power losses for MMC-based VSC HVDC stations. in Power Electronics and Applications (EPE), 2013 15th European Conference on. 2013.

[11] Technical Information, Infineon IGBT Modules F4-50R06W1E3.